RELIABILITY OF DOPED LEAD-FREE SOLDER JOINTS UNDER ISOTHERMAL AGING AND THERMAL CYCLING

Cong Zhao, Thomas Sanders, Chaobo Shen, Zhou Hai, John L. Evans, Ph.D., M.J. Bozack, Ph.D., and Jeffrey Suhling
Center for Advanced Vehicle and Extreme Environment Electronics (CAVE3)
Auburn University
Auburn, AL, USA
czz0025@auburn.edu

ABSTRACT

This paper presents harsh environment reliability test results for lead-free, principally Tin-Silver-Copper (SAC) based, solder pastes with and without the presence of a variety of dopant elements. SAC105 and SAC305 solder alloy spheres are mixed with 12 different doped solder pastes and subsequently tested under long-term isothermal aging and thermal cycling condition in order to evaluate the ability of solder doping to mitigate the effect of aging and to enhance the solder joint reliability. In addition to ball grid arrays (BGAs) with package size ranging from 15mm (0.8mm pitch) to 6mm (0.8mm pitch), the test vehicle also incorporates no-lead packages such as QFNs and 2512 Surface Mount Resistors (SMRs). Three surface platings are tested: Organic Solderability Preservative (OSP), Immersion Silver (ImAg), and Electroless Nickel Immersion Gold (ENIG).

All test vehicles were subjected to isothermal aging at temperatures of 125°C with aging time of either 0 or 12 months, followed by accelerated thermal cycle (ATC) testing from -40°C to 125°C. Previous studies shows reliability of BGA packages can degrade up to 70% after aging at elevated temperature under similar conditions. This paper presents results for the first 1500 thermal cycles. Current reliability data indicates that 8 doped solder pastes demonstrate superior reliability, which can help improving the reliability of lead-free solder under aging, while 4 pastes have somewhat lower performance. Failure analysis shows continuous growth of intermetallic compounds (IMC) at solder joint-pad interface and within solder bulk. Crack propagation is observed in the component-side, near-interfacial region in some materials and through the bulk solder in other materials. 2512 Surface Mount Resistors sampled thus far demonstrate typical fatigue crack propagation mechanics from the inside out through the main fillet.

Key words: lead-free solder, solder paste doping, isothermal aging, reliability, IMC growth

INTRODUCTION

Since 2006, the Europe Union's Restriction of Hazardous Substances (RoHS) restricted the use of leaded solders such as eutectic Sn-37Pb solder in electronics in Europe. Since then, the electronics packaging industry has widely transitioned to lead-free solders. Among many lead-free alloys, Sn-Ag-Cu, or SAC, has become the most popular. A variety of studies have been conducted to investigate the response of lead-free solder materials to isothermal aging and/or thermal cycling environments. Previous research shows that long-term isothermal aging at elevated temperature has a severe impact on the board-level reliability of lead-free solder joints [1-6]. Zhang, et al. [1] observed a significant degradation of up to 70% in the characteristic life of BGA components subjected to thermal cycling following initial isothermal aging for up to 24 months. Significant lifetime degradations were observed for both SAC105 and SAC305 solder joints in 19mm, 15mm, 10mm and 5mm BGA packages, with aging at 25°C, 55°C, 85°C, and 125°C and 6 months, 12 months, and 24 months of isothermal aging. Zhao, et al. [2] investigated this aging effect on the reliability of lead-free solder joints in BGA packages with various ball arrangements. He found that BGA packages with full array ball arrangements were associated with higher reliability under aging than those with perimeter array arrangements. Hai, et al. [3] investigated the reliability of SAC105 and SAC305 solder joints in BGA packages with ImAg, ENIG, and ENEPIG surface finishes with aging at 125°C for up to 12 months. Failure analysis indicated continuous growth of Cu-Sn intermetallic (IMC) in SAC/ImAg solder-plating system, as well as Cu-Ni-Sn IMC in the SAC/ENIG/ENEPIG systems during both thermal aging and cycling. Joint failures were attributed to coefficient of thermal expansion (CTE) mismatch driven thermos-mechanical fatigue, with crack propagation along the near-IMC-interfacial region.

Doping (micro-alloying) has been found to be partially effective in mitigating the effects of aging. Cai, et al. [7] found that adding dopants in SAC solder paste such as Bi, In, Ni, La, Mg, Mn, Ce, Co, Ti, Zn, etc. has become widespread to enhance shock/drop reliability, wetting, and other properties. This approach can be extended to examine the ability of dopants to reduce the effects of aging and enhance thermal cycling reliability. Huang, et al. [8] stated that the addition of Bismuth (Bi) as a dopant has been demonstrated to have several beneficial effects, including improvements in shear strength and reductions of IMC layer thickness in lead-free solder materials.

Since the solder paste is relatively easy to inflect from a manufacturing perspective, the purpose for this project is to find a manufactureable solder paste with dopants that can mitigate the effects of aging. A secondary goal is to find a solder material for solder-sphere replacement to enhance individual package reliability. In this paper, we test a full experimental matrix including various selections of solder alloys, doped solder pastes, package sizes and pitch sizes, surface finishes, isothermal aging time up to 12 months, and isothermal aging temperatures up to 125°C, followed by thermal cycling testing.

EXPERIMENT

The assembled test vehicle consists of a FR4-06 glass-epoxy PCB with a base glass transition temperature of 170°C. The dimensions of the board are 4.0 x 5.0 x 0.062 inches. BGA components are mounted on the PCB using second-level interconnects (solder joints) of paste-doped SAC105 and SAC305, as well as matched doped solder joints (paste and spheres of matching composition) with package sizes of 6mmx6mm, and 15mmx15mm, and 0.8mm pitch size. There are also lead-less ("paste only") QFNs and 2512 surface mount resistors (SMRs) incorporated on the test vehicle, with terminations of 100% Sn. Non-solder mask defined (NSMD) pads were used. Test vehicles with three different surface finishes are tested: OSP, ImAg, and ENIG. The test component matrix is shown in Table 1. Figure 1 shows a schematic of the test vehicle.

Table 1. Test Component Matrix

Package Type	Package Size (mm)	Pitch Size (mm)	Ball Diameter (mm)	Ball Arrangement	Solder Joint
BGA	15x15	0.8	0.46	Perimeter	SAC105 SAC305 MATCH
BGA	6x6	0.8	0.46	Full Array	SAC105 SAC305 MATCH
QFN	5x5	0.65	—	—	Paste Only
2512 Resistor	2.5x1.2	—	—	—	Paste Only

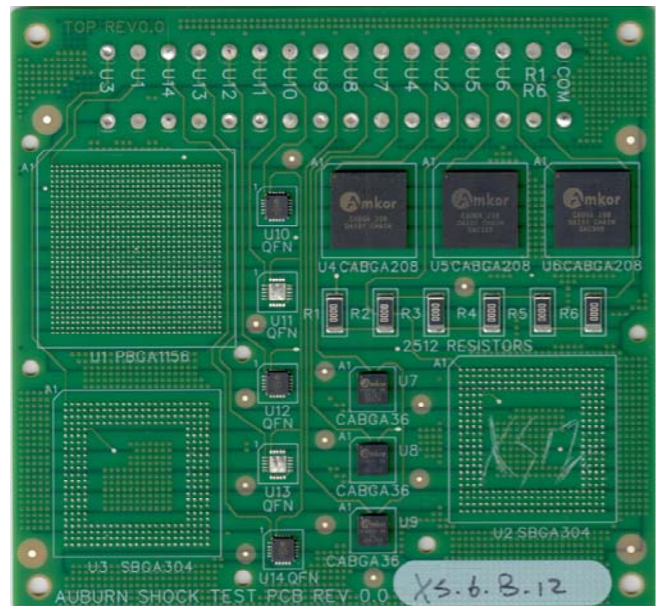

Figure 1. Assembled Test Vehicle.

Table 2, below, shows the thermal aging test plan. 12 solder pastes are tested. These are referenced as Paste A - Paste L. No Aging test vehicles were tested immediately following assembly. All other test vehicles were isothermally aged at 125°C for 12 months.

Table 2. Thermal Aging Test Plan.

Aging / Doped Paste	12 month aging at 125°C			No Aging		
	OSP	ImAg	ENIG	OSP	ImAg	ENIG
Paste A	5	5	5			
Paste B	5	5	5	5	5	5
Paste C	5	5	5	5	5	5
Paste D	5	5	5			
Paste E	5	5	5			
Paste F	5	5	5			
Paste G	5	5	5			
Paste H	5	5	5			
Paste I	5	5	5			
Paste J	5	5	5			
Paste K	5	5	5	5	5	5
Paste L	5	5	5			

Subsequent to aging, all test vehicles were placed vertically in the thermal cycling chamber. The thermal cycling test was from -40°C to 125°C with 15 minutes dwell time and 50 minutes ramp time. Figure 2 shows the thermal cycling profile.

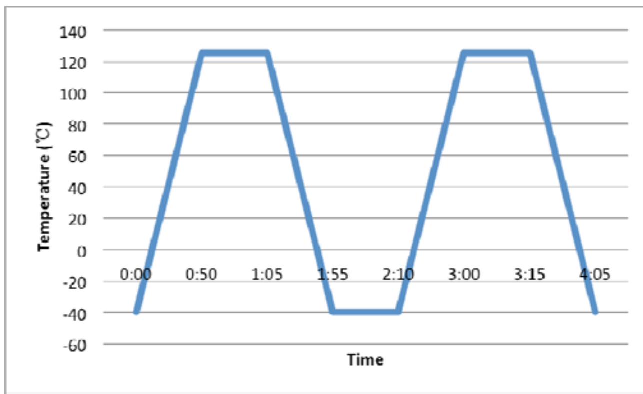

Figure 2. Thermal Cycling Profile.

All test components were wired in daisy-chains, which allowed for continuous sampling of component reliability during accelerated life tests. The daisy-chained components were wired out to a data acquisition developed by Thomas Sanders of Auburn University. This system consists of a switch scanning system coupled with a high accuracy digital multi-meter, which allows for cyclically monitoring the resistance change of each component. In this study, we defined "failure" to occur when the daisy chain resistance increased (from baseline) by over 100 ohms for 5 sequential resistance measurements.

The failure data are reported using two-parameter Weibull analysis and failure percentages. All samples for microscopic examination were cross-sectioned and ground with SiC polishing paper (240, 320, 400, 600, 800, 1200) followed by two-step of polishing with 3 micron diamond suspension. Back-scattered electron micrographs were taken from specimen to do failure analysis.

RESULTS AND DISCUSSION

Data Analysis

Where sufficient failure data is available, the two-parameter (η, β) Weibull distribution has been used to characterize the reliability of electronic packages. The characteristic life η is the point (i.e. number of cycles) at which 63.21% of the population is expected to fail and the slope β relates to the variance of the data and helps distinguish different failure modes. The least squares method was used to estimate the η and β values of the Weibull distribution, and the r^2 value indicates the quality of the data fit.

This project is ongoing, and until the publication of this paper, 1500 thermal cycles have been run. Table 3 shows the failure percentages for each component and surface finish combination for the 12-month aging group. Test groups with complete (100%) failure are shown in red.

Table 3. Failure Percentages at 1500 Cycles.

Component / Doped Paste	12 month aging at 125°C											
	OSP				ImAg				ENIG			
	15mm SAC105	15mm SAC305	15mm Match	2512 Resistor	15mm SAC105	15mm SAC305	15mm Match	2512 Resistor	15mm SAC105	15mm SAC305	15mm Match	2512 Resistor
Paste A	100%	100%	100%	100%	100%	100%	100%	100%	100%	100%	100%	100%
Paste B	0	20%	20%	0	0	0	0	0	0	0	0	0
Paste C	20%	60%	0	0	20%	40%	0	0	0	20%	0	0
Paste D	0	0	0	0	0	0	20%	0	0	0	0	0
Paste E	40%	0	0	0	0	20%	0	0	0	0	0	0
Paste F	40%	0	0	100%	60%	0	20%	100%	20%	20%	0	100%
Paste G	20%	20%	40%	100%	100%	20%	0	100%	20%	0	0	100%
Paste H	60%	20%	0	0	20%	20%	0	0	40%	20%	0	0
Paste I	100%	0	100%	100%	100%	0	100%	100%	100%	0	100%	100%
Paste J	0	0	40%	0	20%	0	0%	0	0	0	0	0
Paste K	20%	0	0	0	0	0	0	0	0	40%	0	0
Paste L	40%	0	0	0	20%	0	0	0	20%	20%	0	40%

No failures have been observed for the No Aging test group. Also no failure occurred for 6mm BGA and QFN components across all test groups. This corresponds to the standard DNP scaling relationship and also matches with research by Zhao, el al. [2], which mentioned that BGA with full array ball arrangement tends to have much higher reliability than perimeter array.

Based on Table 3, we can conclude that Paste A performs worst for all test components. For Paste I, it only performs well with SAC305 solder sphere BGA. And for Paste F and Paste G, applying them with 2512 resistor can cause reliability issues. So for all test components applications, we select Paste B, Paste C, Paste D, Paste E, Paste H, Paste J, Paste K, and Paste L as primary candidate for best material. If it deals with only BGA application, Paste F and Paste G may also be considered as good candidates.

Weibull plots have been generated for comparing characteristic life of reliability of Paste A, Paste F, Paste G, and Paste I. Figure 3 shows Weibull plots for 15mm BGA with Paste A on each surface finish. Figure 4 shows Weibull plots for 2512 Resistor with all 4 pastes on each surface finish.

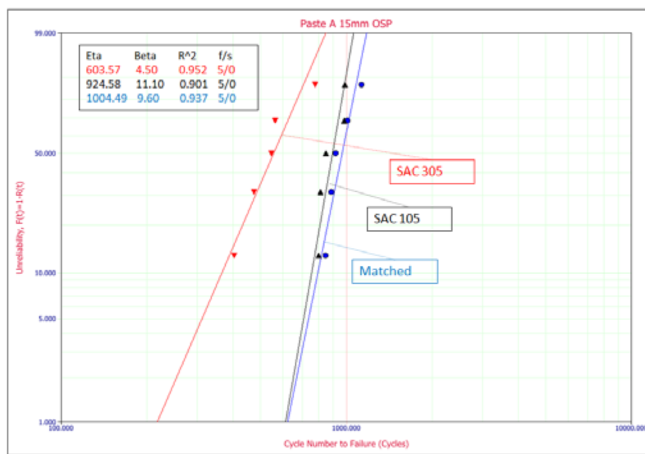

(a)

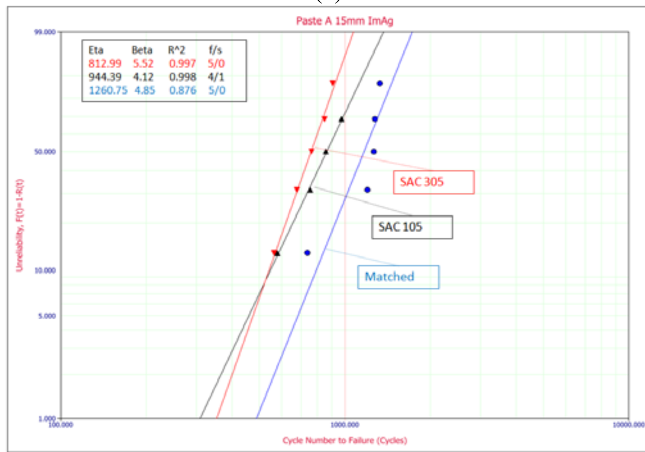

(b)

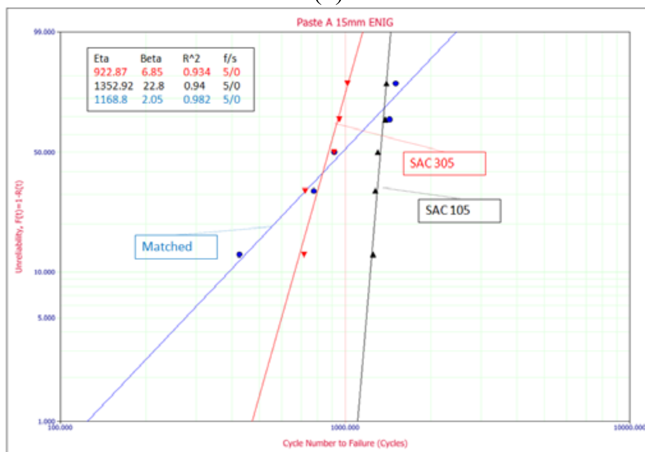

(c)

Figure 3. Weibull plots for 15mm BGA with Paste A on each surface finish: (a) OSP, (b) ImAg, (c) ENIG.

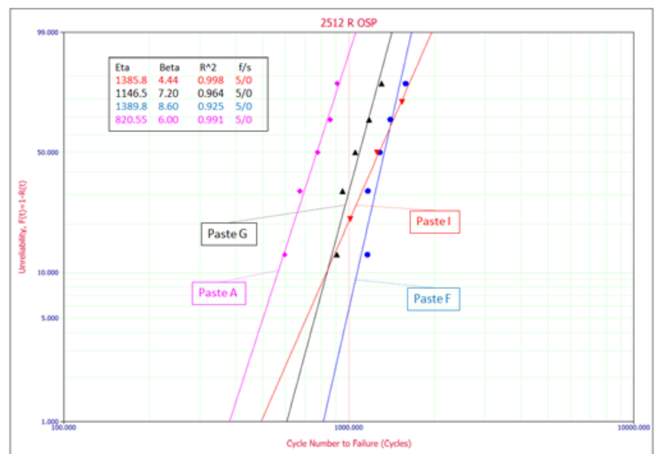

(a)

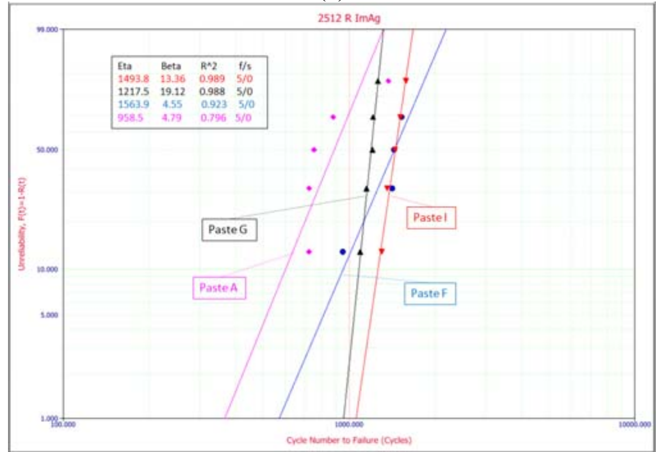

(b)

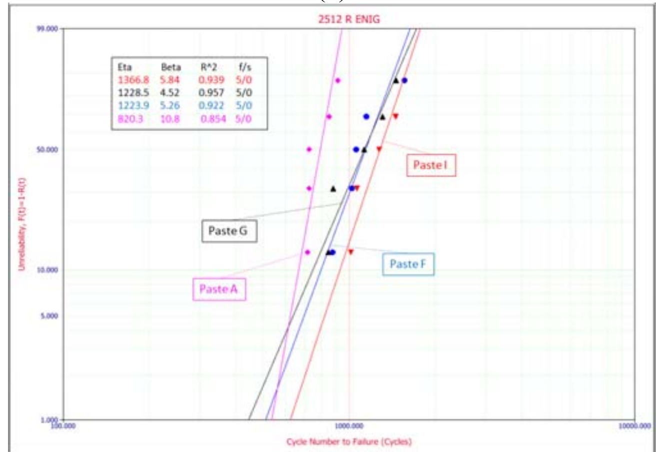

(c)

Figure 4. Weibull plots for 2512 Resistor with all 4 pastes on each surface finish: (a) OSP, (b) ImAg, (c) ENIG.

To present the data more succinctly, we have summarized the characteristic life values for all subgroups based on the Weibull fittings. Figure 5 shows the characteristic life values for the 15mm BGA with Paste A.

Figure 5. Characteristic Life values for 15mm BGA with Paste A.

From Figure 5, we can conclude that for Paste A, the matched composition joints perform generally better (with an exception for the ENIG finish) than the paste-doped SAC joints. Considering paste doping of SAC105 and SAC305, for material A, doped SAC105 joints always outperform doped SAC305 joints. Doped SAC305 joints are found to have lower characteristic life than both the matched Material A joints and doped SAC105 joints in all cases.

Figure 6 shows the characteristic life value comparison for Paste A, Paste F, Paste G, and Paste I with 2512 Surface Mount Resistors.

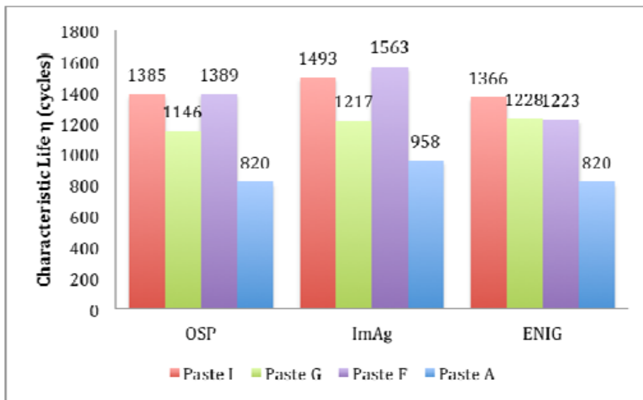

Figure 6. Characteristic Life values for 2512 SMR with Paste A, Paste F, Paste G, and Paste I.

From Figure 6 we can conclude that, for the "paste only" SMR components, Paste A has the worst reliability in all cases. The best two materials overall (from this group of four) appear to be Paste I and Paste F. Paste G performs better than Paste A, but generally worse than Pastes I and F.

Failure Analysis

During thermal aging and cycling, the solder joint undergoes microstructure evolution and deformation [9-11]. Typically, the coefficient of thermal expansion (CTE) mismatch between the printed circuit board (PCB) and the component drives the fatigue failures within the solder joints. Microstructural changes in the solder joints, including intermetallic compounds (IMC) layer thickening at joint-pad interfaces of primary and secondary precipitates also contribute to degradations in the joint's mechanical properties. Grain coarsening and – in certain cases – dynamic recrystallization processes are often implicated in the crack formation and propagation processes [12].

Figure 8 shows typical BGA solder joint failure modes observed so far in this study. Crack propagated either along both board and package side near-interfacial region (Figure 8.a), or through the bulk of the solder joint (Figure 8.b).

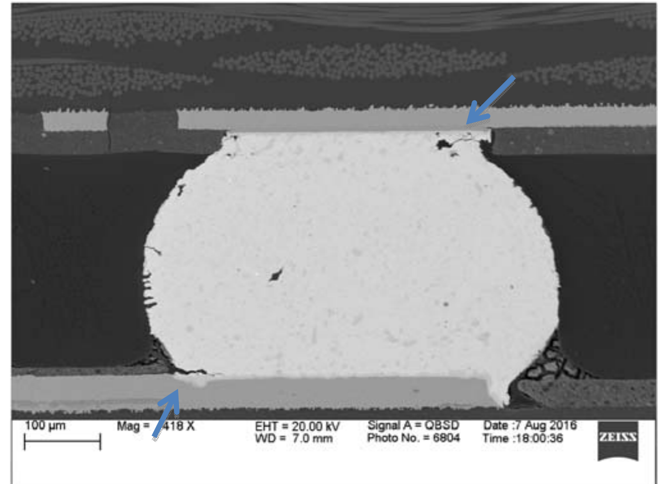

(a)

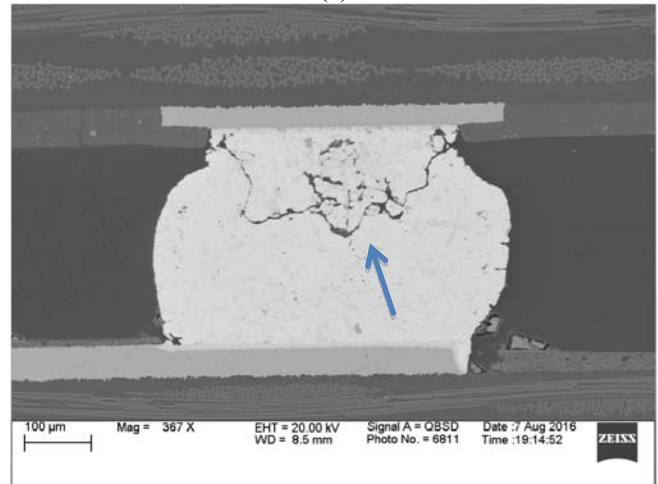

(b)

Figure 8. Representative solder joints failure modes. Crack propagation close to the (a) board-side and package-side IMC layer. (b) Crack propagation through the solder bulk.

During thermal aging and cycling, IMC layer in both the component- and board-side interfaces thicken continuously, consuming material from the copper pads and solder joint. The near-interfacial region is often the principal area in which crack initiation and propagation are observed due to high stress concentration and fatigue caused by CTE mismatch. Higher ductility materials, however, have lower stress concentrations and are more likely to see the bulk failure mode shown in Figure 8 (b). Dynamic

recrystallization has been theorized to play a role in this type of crack propagation [13].

Figure 9 shows SEM micrographs of solder joint composed of Paste I with SAC105 (a) prior to thermal cycling and (b) after 1500 thermal cycles. Board-side average IMC thickness is 4.9 μm prior to cycling, and 7.4 μm after 1500 thermal cycles. Aggressive IMC thickening during thermal cycling of joints composed of Paste I with SAC105 indicates that the dopants and/or doping levels involved are not sufficient to stabilize the interfacial IMC layers.

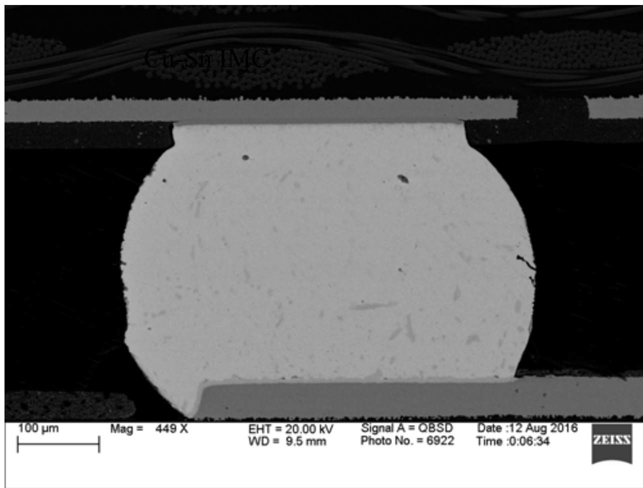

(a)

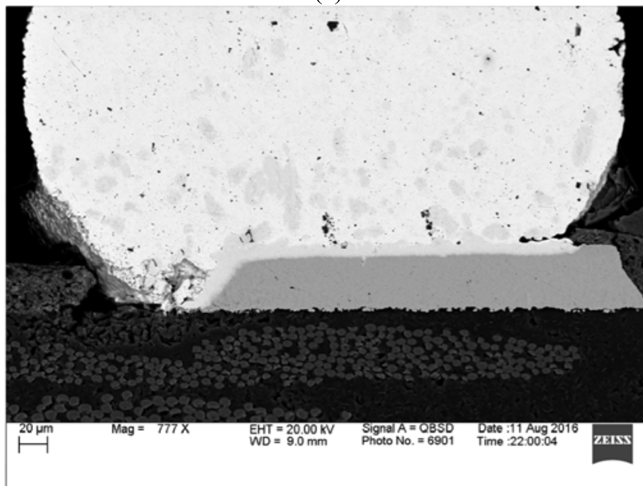

(b)

Figure 9. SEM micrographs of solder joint composed of Paste I with SAC105 (a) prior to thermal cycling and (b) after 1500 thermal cycles.

Figure 10 shows the typical solder joint failure mode for 2512 Resistor. We can find crack initiates at the inside of the joint and propagates underneath the component termination and then outward through the primary fillet until an open circuit occurred. This is the typical fatigue failure mechanism observed in surface mount resistors. Crack initiation generally occurs in high stress regions, which for surface mount resistors are located beneath the termination.

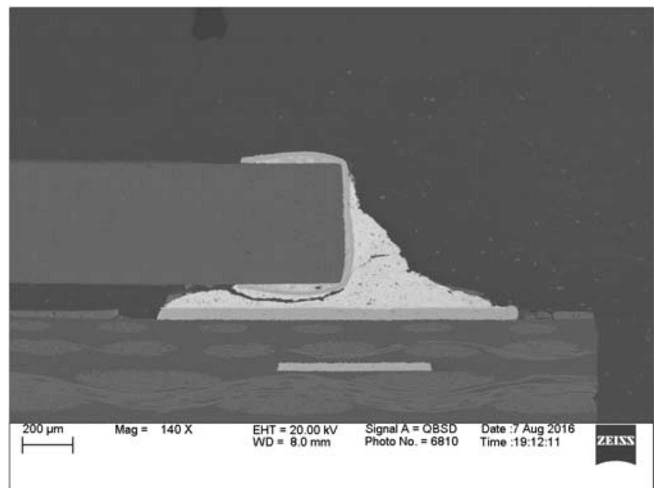

Figure 10. Typical failure mode for 2512 SMR.

CONCLUSIONS

In this experiment we have investigated 12 different doped solder pastes in combination with a variety of different components and surface finishes. Test vehicles were subjected to long-term isothermal aging and thermal cycling conditions in order to evaluate the viability of solder doping for enhancing solder joint reliability. Based on data analysis at 1500 thermal cycles, 8 doped solder pastes demonstrate superior reliability, while 4 pastes have somewhat lower performance. Current failure percentages indicate that, Paste A is the least reliable of all solder pastes, following paste I. Paste F and G also have poor reliability performance when used with 2515 Surface Mount Resistors. Failure analysis shows thermal-mechanical fatigue failures. BGA joints exhibit crack propagation either along the near-IMC interfacial regions or within the solder bulk. Pastes that have bad reliability performance have significant IMC thickening, with copper diffusion from the copper pads apparently undeterred by doping. For 2512 Resistor, cracks were found to initiate underneath the component, and then propagate out through the primary fillet until an open circuit occurred.

ACKNOWLEDGEMENTS

This work was supported by the Center for Advanced Vehicle Electronics and Extreme Environment Electronics (CAVE3).

REFERENCES

[1] J. Zhang, Z. Hai, S. Thirugnanasambandam, J.L. Evans, M. J. Bozack, "Correlation of Aging Effects on Creep Rate and Reliability in Lead Free Solder Joints," Journal of Surface Mount Technology, (2012). Vol. 25 (3), pp. 19-28 Orlando, FL.

[2] C. Zhao, C. Shen, Z. Hai, M. Basit, J. Zhang, M. J. Bozack, J.L. Evans, J. C. Suhling , "Long Term Aging Effects on the Reliability of Lead Free Solder Joints in Ball Grid Array Packages with Various Pitch Sizes and Ball Arrange," Journal of Surface Mount Technology, Vol. 29 (2), pp. 37-46, 2016

[3] Z. Hai, J. Zhang, Chaobo Shen, J. L. Evans, M. J.

Bozack, " Long Term Aging Effects on Reliability Performance of Lead-Free Solder Joints," proc. Surface Mount Technology International Conference, 2013.
[4] S. Sridhar, A. Raj, S. Thirugnanasambandam, J. L. Evans, “Drop Impact Reliability Testing of Isothermally Aged Doped Low Creep Lead-free Solder Paste Alloys,” Proceedings of ITherm 2016, pp. 501-506, 2016.
[5] J. Gong, I.C. Ume, et al. "Non-Destructive Evaluation of Solder Bump Quality Under Mechanical Bending Using Laser Ultrasonic Technique", Journal of Surface Mount Technology , vol.28, Issue 3, PP15-25, Aug. 2015
[6] M. A. Matin, W. P. Vellinga, M. G. D. Geers. “Thermomechanical Fatigue Damage Evolution in SAC Solder Joints,” Materials Science and Engineering A 445–446, pp. 73–85, 2007.
[7] Cai, Z., Zhang, Y., Suhling, J. C., Lall, P., Johnson, R. W., Bozack, M. J., “Reduction of Lead Free Solder Aging Effects using Doped SAC Alloys,” Proceedings of the 60th Electronic Components and Technology Conference, pp. 1493-1511, Las Vegas, NV, June 1-4, 2010.
[8] Huang, M. L. and Wang, L., “Effects of Cu, Bi and In on Microstructure and Tensile Properties of SnAg-X (Cu, Bi, In) Solders,” Metallurgical and Materials Transactions A , Vol. 36(6), pp. l439-1446, 2005.
[9] M. Berthou, P. Retailleau, H. Frémont, A. Guédon-Gracia, and C. Jéphos-Davennel, “Microstructure evolution observation for SAC solder joint: Comparison between thermal cycling and thermal storage,” Microelectron. Rel., vol. 49, nos. 9–11, pp. 1267–1272, Sep./Nov. 2009
[10] J. Gong, I.C. Ume, " Nondestructive Evaluation of Poor-Wetted Lead-free Solder Joints in Ball Grid Array Packages using Laser Ultrasound and Interferometric Technique", Components, Packaging and Manufacturing Technology, IEEE Transactions on , vol.3, no.8, pp.1301,1309, Aug. 2013
[11] J. W. Yoon, B. I. Noh, J. H. Yoon, H. B. Kang, S. B. Jung, “Sequential Interfacial Intermetallic Compound Formation of $Cu_6Sn_5$and Ni_3Sn_4between Sn-Ag-Cu Solder and ENEPIG Substrate During a Reflow Process,”J. Alloys and Compounds509, pp. L153-L156, 2011
[12] B. Vandevelde , M. Gonzalez, P. Limaye, P. Ratchev, E. Beyne, “Thermal cycling reliability of SnAgCu and SnPb solder joints: A comparison for several IC-packages,” Microelectronics Reliability 47 (2007) 259–265
[13] H. Chen, M. Mueller, T. T. Mattila, J. Li, X. Liu, K. J. Wolter, P. K. Mervi, “Localized recrystallization and cracking of lead-free solder interconnections under thermal cycling”,J. Materials research, vol. 26, No. 16, pp. 2103-2116, 2011.